Characterization of the ultrafast carrier dynamics of an InAs/InGaAsP quantum dot semiconductor optical amplifier operating at 1.55 μm

Aaron J. Zilkie*, Joachim Meier, Peter W. E. Smith, Mohammad Mojahedi, J. Stewart Aitchison
Edward S. Rogers Sr. Department of Electrical and Computer Engineering,
University of Toronto,10 King's College Rd. Toronto, ON, Canada M5S 3G4

Philip J. Poole, Claudine Nì. Allen, Pedro Barrios, Daniel Poitras
Institute for Microstructural Sciences, National Research Council, Building M-50, Montreal Road
Ottawa, ON, Canada K1A 0R6

ABSTRACT

Self-assembled quantum dot (QD) Semiconductor Optical Amplifiers (SOAs) are believed to have faster carrier recovery times than conventional multiple quantum well, or bulk SOAs. It is therefore of interest to study the carrier dynamics of QD SOAs to assess their potential as ultrafast nonlinear devices for switching and signal processing. In this work we report experimental characterization of the ultrafast carrier dynamics of a novel InAs/InGaAsP self-assembled QD SOA with its peak gain in the important 1.55 μm telecommunications wavelength range. The temporal dynamics are measured with a heterodyne pump-probe technique with 150 fs resolution. The measurements show carrier heating dynamics with lifetimes of 0.5-2.5 ps, and a 13.2 ps gain recovery, making the device a promising candidate for ultrafast switching applications. The results are compared to previous reports on QD amplifiers operating in the 1.3 μm and 1.1 μm spectral regions. This report represents the first study of the temporal dynamics of a QD SOA operating at 1.55 μm.

Keywords: Semiconductor quantum dots, quantum dot amplifiers, semiconductor optical amplifier, heterodyne pump-probe, ultrafast, carrier, nonlinear, dynamics, carrier heating, all-optical switching.

1. INTRODUCTION – APPLICATIONS TO ALL-OPTICAL SIGNAL PROCESSING

For communications systems to evolve beyond the speed limitations of the electronics domain, time division multiplexing and signal processing entirely in the optical domain is needed. All-optical signal processing devices operating at speeds > 40 Gb/s would represent a significant advancement impacting a wide range of applications in communications, computing, and signal processing. All-optical devices should ideally be easily integratable with passive optical waveguides and other optical devices, be small in dimensions, easy to manufacture, and cascadable into larger circuits. Switches constructed using a semiconductor optical amplifier (SOA) as a nonlinear element, monolithically integrated into an interferometer structure, are very promising because they would possess all of these attributes. In these devices the resonant ultrafast dynamics in the SOA have an almost instantaneous nonlinear response that is large enough to allow for switching over the short distances of typical SOA device lengths. However, much design and engineering of SOAs and semiconductor waveguide structures remains to be done to make these devices practical. Quantum dot (QD) and other nanostructured SOAs have very recently attracted attention because they have been shown to be able to provide switching at speeds of 10, or up to 100 times faster than quantum-well or bulk SOA structures [3-8]. QD SOAs have been also found to have improved nondegenerate four-wave-mixing (FWM) properties over well and bulk structures [9]. Also, due to recent revolutionary work on QD lasers, QD active guided-wave device fabrication has become well developed. QDs are being embedded in the active layer of waveguides via Stranski-Krastanov (SK) growth, the technique of self-assembly under strained growth during Molecular Beam Epitaxy (MBE) [10]. Thus QD laser and amplifier devices can be made using common III-V semiconductor material systems, using already established growth techniques, through well understood and reproducible processes. With these combined

* Email: aaron.zilkie@utoronto.ca *Tel: (416) 946-8663 Fax: (416) 971-3020 http://photonics.light.utoronto.ca/aitchison/*

attributes, QD SOAs are becoming an attractive solution for high-bit-rate and multi-wavelength optical signal processing, providing for devices with the potential to work as all-optical time-division multiplexers, wavelength converters, and regenerators.

All-optical switching devices have been demonstrated using SOAs as non-linear elements in various different structures. Amongst the most promising are interferometric structures based on cross-phase modulation (XPM), for example a Mach-Zehnder Interferometer structure, or TOAD structure [11]. Other interesting XPM-based switching schemes are the Ultrafast Nonlinear Interferometer (UNI) [12], and the delayed interference (DI) configuration [13,14]. A delayed interference scheme was demonstrated in 2001 to perform all-optical switching at 100 Gb/s with 13dB extinction ratio. Finally, switching schemes can also be based on cross-gain modulation (XGM), and four-wave mixing (FWM). Regardless of the nonlinear process used however, the important engineering parameter is the fundamental limit of the SOA gain and refractive index recovery times. Once a bit switch is performed, it can not be effectively repeated until the nonlinearity change (the phase change in XPM schemes, gain or absorption change in XGM schemes, or $\chi^{(3)}$ change for FWM) has recovered back to the equilibrium state. Therefore assessing the ability of QD materials in SOA-based ultrafast (>40 Gb/s) signal processing requires a detailed understanding of the SOA ultrafast dynamics. Quantum dot (QD) SOAs are believed to have recovery times with values less than 10 ps [15,16], as compared to multiple quantum well (MQW) devices with measured recovery times of 60 to 150 ps, or larger [17,18]. In this report we present an experimental characterization of the ultrafast dynamics of a novel InAs/InGaAsP 1.55 μm QD SOA, to assess its potential as a nonlinear element in ultrafast XPM- or XGM-based all-optical signal processing. These measurements are also the first measurements of the dynamic behavior of an active semiconductor QD device operating in the important 1.55 μm telecommunications wavelength range, and are thus important for investigating the characteristics of this important class of devices.

2. SAMPLE AND EXPERIMENT

2.1. QD sample and gain characteristics

The QD sample measured is the 1.55 μm InAs/InGaAsP QD laser device reported in [19], with the end-facets anti-reflection coated to suppress lasing and create a single-pass amplifier. The structure is a p-i-n doped ridge-waveguide diode grown by chemical beam epitaxy on an InP substrate, and cleaved into 1-mm length bars. Their undoped active region consists of five stacked layers of self-assembled (SK-grown) InAs dots embedded in InGaAsP. The devices come from wafer "B" of the three types mentioned in [19], having a 400 nm thick undoped core with a $1.5\times10^{10}\,\mathrm{cm}^{-2}$ dot planar density, and a quaternary composition of $In_{0.816}Ga_{0.184}As_{0.392}P_{0.608}$, thus providing a high energy barrier for the QDs. The wafer structure is outlined in Table 1, and an SEM image of the QDs in the core region is shown in Figure 1.

Figure 2 shows the spectral and gain properties of the device, characterized with laser light from a 150 fs-pulse

Material	#	Thickness	Doping		Ga %	As %	Strain %
wafer epitaxial surface							
InGaAs	1	200 nm	1e19	Mg	47.8	100	0.07%
InP	1	1.2 um	5e17	Mg	0	0	0
InGaAsP	1	10 nm		undoped	26	57	0
InP	1	200 nm	5e17	Mg	0	0	0
InGaAsP	1	150 nm		undoped core	18.4	39.2	0
InAs (SK dots)	5	0.9 nm		undoped core	0	100	-3.1
InGaAsP	5	25.4 nm		undoped core	18.4	39.2	0
InGaAsP	1	125 nm		undoped core	18.4	39.2	0
InP	1	600 nm	1e18	Si	0	0	0
InP substrate							

Table 1 – Wafer structure of the 1.55 μm InAs/InGaAsP QD SOA measured in this work.

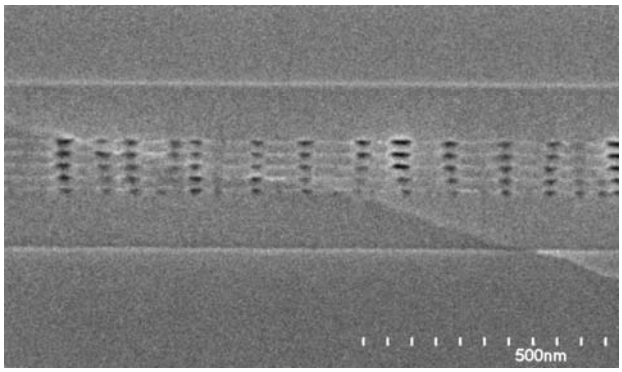

Figure 1 – SEM image of the 1.55 μm InAs/InGaAsP QD SOA wafer.

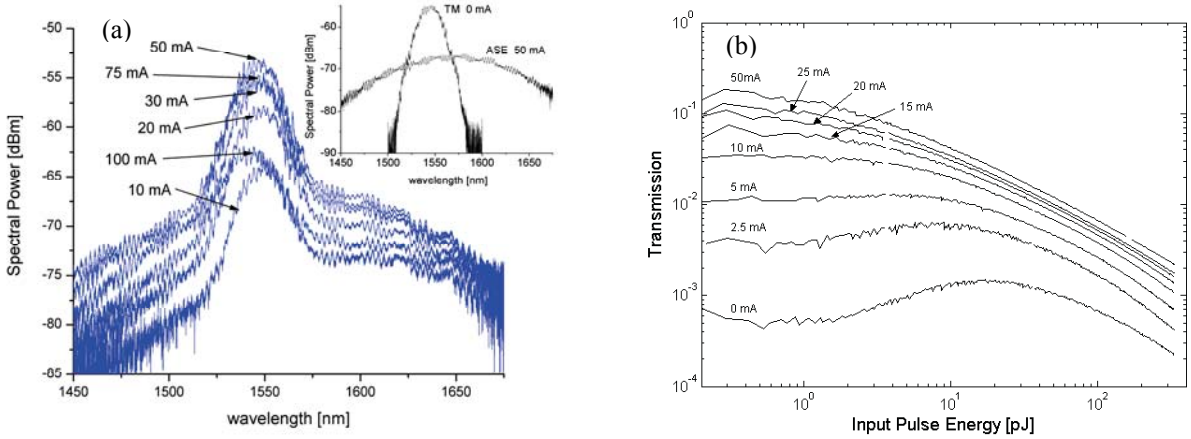

Figure 2 – Gain and spectral characteristics of the measured QD SOA; (a) Output spectra of TE-polarized OPO light amplified for varying bias currents. Maximum gain occurs at 50 mA; Inset: ASE spectrum for 50mA bias current, and TM spectrum with no bias current (SOA transparent), illustrating laser spectrum; (b) Transmission vs. input pulse energy showing absorption and gain saturation and onset of nonlinear absorption.

optical parametric oscillator (OPO) at 1550 nm (the same used for the main experiment described in section 2.2). Figure 2 (a) shows the spectra of the amplified TE-polarized OPO light for increasing bias currents. The inset additionally shows the spectrum of the OPO light passing through the device unattenuated in the transparent TM polarization state, overlayed with the ASE spectrum of the device at 50 mA bias. The OPO spectrum is near the peak of the ASE spectrum and thus near the gain peak of the SOA, a requirement for characterizing the ground-state transition of the QD ensemble. The large ASE bandwidth is a result of inhomogeneous broadening due to the size distribution of the QDs, and is typical for self-assembled QD lasers and amplifiers. In the TE polarization state the OPO light experiences resonant absorption and gain, as seen by the increasing peak of the OPO spectrum as the bias current is increased. Maximum gain is achieved with a 50 mA bias current, since it is seen that for higher currents (75 and 100 mA) a reduction in gain occurs due to saturation. Figure 2 (b) summarizes the gain characteristics, showing a plot of transmission versus input pulse energy for bias currents up to 50 mA. The transmission in the plot is the transmission from the input coupling lens to the output coupling lens, including stimulated absorption/gain, as well as the modal coupling loss between the waveguide mode and focused laser beam mode, and other fixed waveguide losses. The coupling lens insertion losses were estimated and calibrated out of the values. The curves are thus proportional to the net absorption, or gain, of the device, and reveal absorption and gain saturation as a function of input pulse energy. The transparency current, the current at which the modal gain exactly equals the linear absorption in the active region, was estimated to be near 25 mA and was deduced from the pump probe traces. For currents below the transparency current, the SOA is in the absorption regime, and for currents above, in the gain regime. It can be seen in the figure that for low

(small-signal) input pulse energies, in all regimes, the absorption/gain is linear and the transmission remains flat. However as the pulse energies increase above approximately 2 pJ, gain and absorption saturation (bleaching) begins to occur. In the absorption regime this results in an increase in transmission, and in the gain regime a decrease in transmission. Then as the input energies increase even further, nonlinear absorption (two-photon absorption) becomes dominant, resulting in a steady decrease in transmission at all current levels (see also [20]).

2.2. Heterodyne pump-probe experiment

The critical temporal responses of an SOA that influence its switching performance are i) the carrier recovery lifetime, which limits the time duration between consecutive switch operations, and ii) the ultrafast responses near zero time delay, which perturb the ideal instantaneous step response and dictate the shape of the switching window and the quality of the extinction ratio. To characterize these dynamics, the pump-probe experimental technique is used. The basic concept of the technique is to use two synchronized optical beams of short-duration pulses, one as a pump to induce a response, and one as a probe which samples the changes in transmission of the material as a function of pump-probe delay. The duration of the pulses dictate the resolution of the measurement, and the time between pulses (i.e. the laser repetition rate) must be longer than the time needed for the dynamics induced by the previous pulse to completely recover. The remaining criteria is for the pump and probe pulses to be orthogonal when overlapping in space and time. The probe pulses must only respond to the change in the medium due the presence of the pump pulses, and not directly to the presence of the pump pulse itself (i.e. via interference with the pump). This is most simply achieved using orthogonal polarizations for the pump and probe beams, however this has the significant disadvantage that it can not properly characterize devices that have a polarization anisotropy in their gain response. Such a polarization anisotropy is an inescapable property of quantum well and quantum dot structures which introduce directionally-dependant quantization in the active region. The heterodyne pump-probe setup was developed by K. Hall et. al. in the mid 1990s [21,22] as the solution to measuring polarization dependant devices, to avoid pump and probe interaction during walk-off at zero-delay, and as well to provide the ability to measure both gain and phase changes simultaneously. The technique was advanced further by P. Borri et al. in [23], and has since then been used extensively to characterize the ultrafast temporal dynamics in semiconductor lasers and amplifiers [15,16,24-27].

Our heterodyne setup constructed for the measurements in this report is similar to that described in [16], and a schematic is shown in Figure 3. The laser source used for the measurements was a Ti:sapphire pumped optical parametric oscillator (OPO), providing nearly Fourier-limited 150 fs pulses at a repetition rate of 76 MHz, tuned to the 1550 nm SOA gain peak. To perform the heterodyne measurements the laser is split into three beams, pump, probe, and reference. Acousto-optic modulators (AOMs) upshift the center frequency of the probe and reference beams, by 53.5 MHz and 52 MHz respectively. The three beams are then recombined collinearly and coupled using microscope objectives into the SOA device under test. The three beams are combined such that the reference pulses lead the probe pulses by a fixed delay of approximately 4.4 ns. Additionally the pump beam travels through a variable delay stage, so that the pump pulses are delayed an adjustable time τ_p from the probe pulses. At the output of the device under test, the pulse triplets are passed through an unbalanced Michelson interferometer, such that the probe pulses are temporally recombined with the reference pulses ('undoing' the 4.4 ns time delay). The probe and reference pulses will then beat at their difference frequency, 1.5 MHz, and this beat signal is detected by an RF lock-in amplifier. Note that the reference pulses pass through the sample before the pump pulses in all cases, and therefore remain unchanged in amplitude and phase. Pump-induced changes in the probe transmission will change the ratio of the probe pulses' amplitudes to the fixed reference pulses' amplitudes, which will change the amplitude of the probe-reference beat and will register as a change in the $R = \sqrt{X^2 + Y^2}$ component of signal detected by the lock-in amplifier. Similarly pump-induced changes in the refractive index will change the phase of the probe pulses with respect to the fixed reference pulses' phase, which will change the phase difference between the probe-reference beat and the lock-in reference signal from the OPO laser. This will be detected as a change in the $\theta = tan^{-1}(Y/X)$ component measured by the lock-in amplifier. Thus by monitoring the R and θ signals from the lock-in amplifier as the pump-probe delay is swept in time, the amplitude and phase dynamics of the sample are measured with a resolution equal to the laser pulse-width. A detailed description of the theory of the heterodyne technique is given in [28].

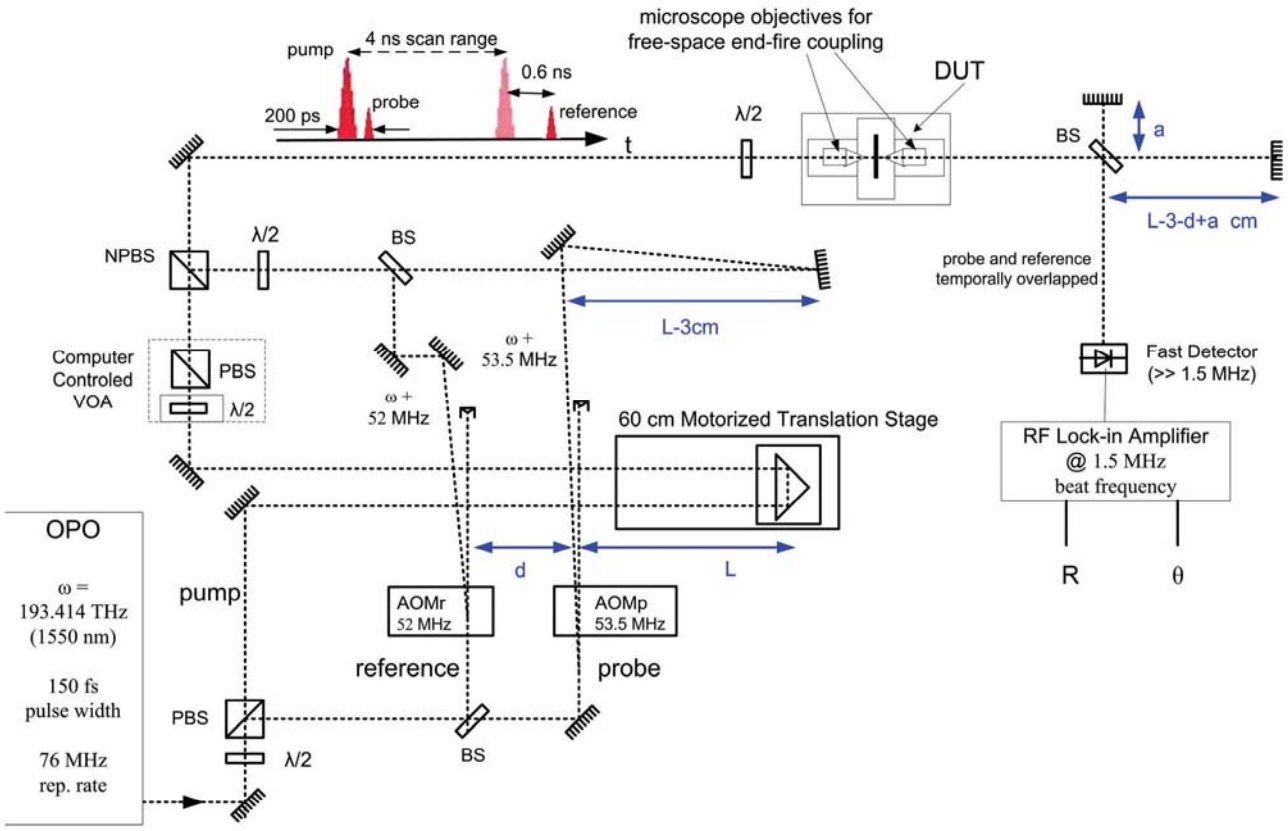

Figure 3 – Schematic of the heterodyne pump-probe experimental setup used for our measurements. (λ/2) = half-wave plate, (PBS) = polarization beam-splitting cube, (BS) = beam splitter, (AOM) = acousto-optic modulator, (NPBS) = non-polarizing beam-splitting cube, (VOA) = variable optical attenuator, (DUT) = device under test.

3. EXPERIMENT RESULTS

Pump-probe measurements were performed as described in section 2.2, with pump, probe, and reference beams in the TE polarization, and tuned to 1550 nm (as in Figure 2). The pump and probe input pulse energies were 7.5 pJ and 0.65 pJ respectively, giving a pump-probe power ratio of ~10. The reference beam pulse energy was set to equal that of the probe. Referring to Figure 2 (b), a 7.5 pJ input pump pulse energy is well into the absorption/gain saturation regime, so as to induce carrier population changes, while the 0.65 pJ probe energy is in the small-signal regime. The measurements then reveal the dynamics of the long-lived carrier density changes which have lifetimes on the order of tens to hundreds of picoseconds, as well as the short-lived picosecond dynamics, on the order of a picosecond, or less. The short-lived responses have been consistently observed in previous measurements of quantum-confinement-based semiconductor structures [2,5,15,16,20,24,25,29], and have been explained phenomenologically to be attributed to two-photon absorption (TPA), spectral hole burning (SHB), and carrier heating (CH). Example responses from a quantum well SOA from [2] are shown in Figure 4 to illustrate typical dynamics. The responses depend on which regime the SOA is biased in: absorption, transparency, or gain. In the absorption regime, electron-hole pairs (excitons) are created in the QD ground state, and the carrier density increases in response to the pump pulse. This results in absorption bleaching which induces in a step increase in probe transmission. The electron-hole pairs then recombine through spontaneous carrier recombination, giving exponential decay in the transmission back to the unperturbed equilibrium state with a lifetime time τ_{cr}. In the gain regime, stimulated emission dominates over absorption, pump-induced

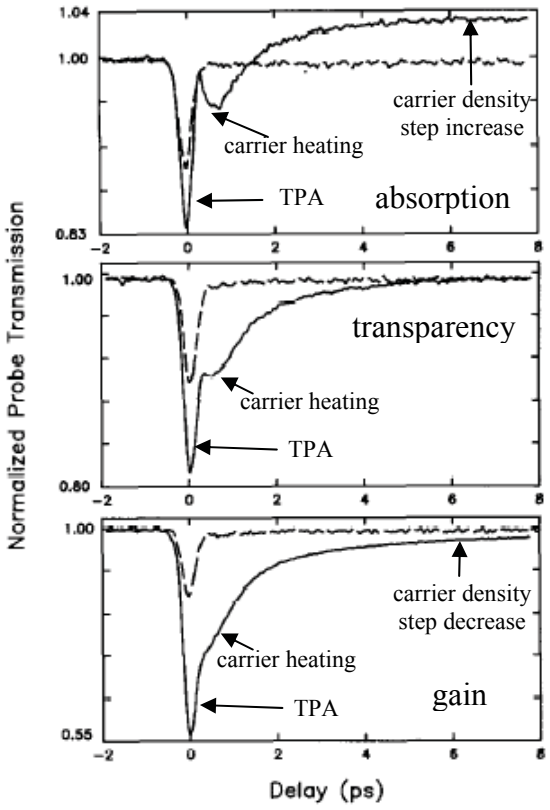

Figure 4 – Example gain dynamics from pump-probe measurements on an InGaAs/InGaAsP SLMQW diode from [2], showing the gain, transparency, and absorption regimes. Also shown are the expected TPA and carrier heating (CH) ultrafast dynamics, and the step changes due to the long-lived carrier density changes.

stimulated emission reduces the exciton population, and a subsequent probe pulse experiences a reduction in gain. The gain then recovers exponentially with time constant τ_{gr} as the exciton population is replenished via relaxations from excited states. Lastly, in the transparency regime the gain exactly compensates for absorption, and there is no step carrier density change. Figure 4 also shows the short-lived perturbations attributed to two photon absorption and carrier heating. The initial instantaneous decrease in probe transmission is attributed to two-photon absorption (TPA) because it has no measurable time constant, matches closely with the autocorrelation trace of the laser pulses, and is only weakly dependent on injected current and pump-probe wavelength. The additional dynamic with a recovery of approximately 1.5 ps is attributed to carrier heating [2,15]. Here stimulated transitions and free carrier absorption induced by the pump heat the carrier distributions (by removing 'cold' carriers below the average carrier energy and creating 'hot' carriers above the average energy). The heated distributions then cool back to the lattice temperature on a picosecond timescale through emission of longitudinal optical phonons. The results of our measurements are shown in Figure 5. Long-range, low time-resolution measurements over the full pump delay translation range (4 ns) were taken to reveal any long-lasting carrier population dynamics, as well as short-range high resolution measurements (over 10 ps) to characterize the ultrafast dynamics. Figure 5 (a) shows the long range responses obtained, together with exponential fits to the data (dotted lines), and Figure 5 (b) shows the short range responses, with their exponential fits. The long-range responses were fitted to a single exponential, multiplied by a step function at zero-delay: $h_{ir}(t) = u(t)k_{cr}e^{-t/\tau_{cr}}$. At 5-25 mA bias the traces show a step increase in transmission indicative of the absorption regime, followed by a exponential decay of approximately τ_{cr} = 500 ps. Figure 6 (a) shows τ_{cr} for the exponential fits versus bias current. This 500 ps spontaneous recombination time matches the recombination lifetimes previously observed in InAs/AlGaAs QDs [16]. The 50 mA curve in Figure 5 shows a step decrease in transmission indicative of the gain regime. It shows a recovery time of only

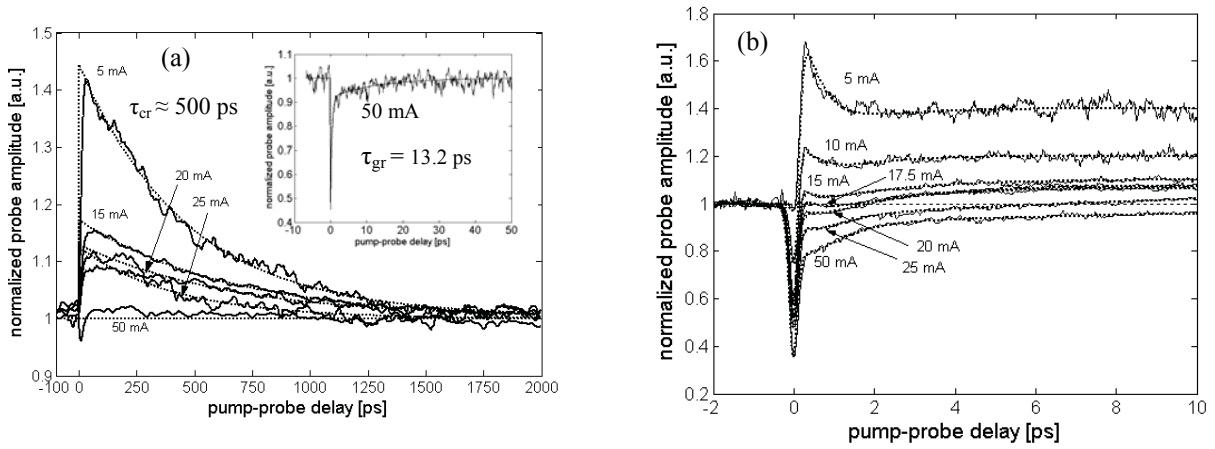

Figure 5 – Long-range (a) and short-range (b) gain dynamics from our measurements on the 1.55 µm QD SOA. Dotted lines show exponential fits. The inset in (a) shows a magnification of the 50 mA trace from 0 to 50 ps.

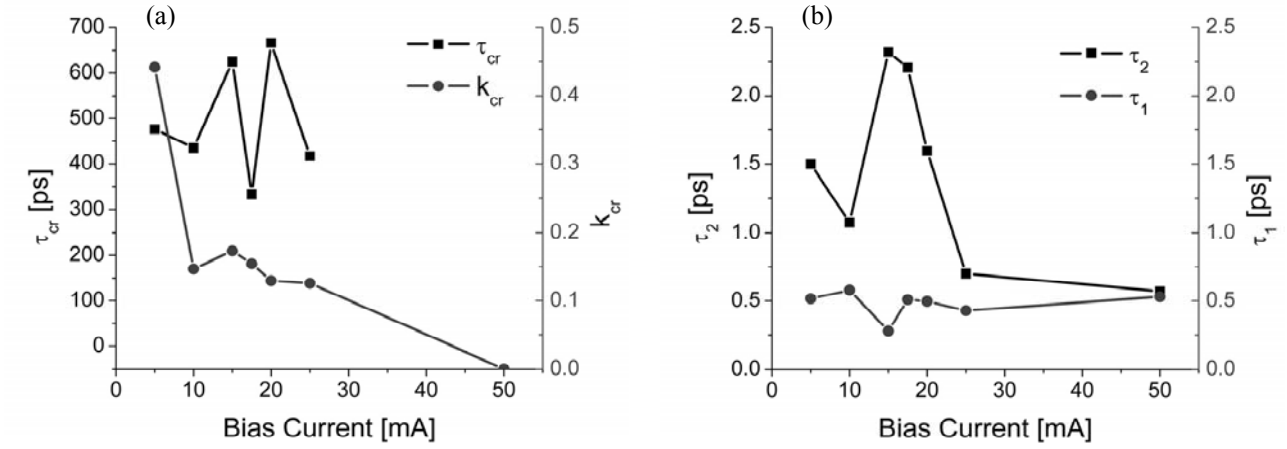

Figure 6 – Values of the time constants of the exponential fits to the curves in Figure 5 v.s. bias current.

13.2 ps however, much shorter than in the absorption regime, and only visible in a higher-resolution scan (see inset of Figure 5 (a)). The transparency current is deduced to be between 25mA and 50mA, likely near 25mA.

The short-range responses revealing the ultrafast dynamics around zero delay clearly show TPA and CH dynamics similar to those observed and discussed in [2]. Thus the dynamics can be fitted to a phenomenological model involving an impulse response function *h(t)* for the SOA that is a series of exponentials [2]:

$$h(t) = h_{TPA} + h_{cr} + h_{ch} + 1, \tag{1}$$

$$h_{TPA} = k_{TPA} u(t) \delta(t), \tag{2}$$

$$h_{cr} = k_{cr} u(t), \tag{3}$$

$$h_{ch} = u(t)\left(k_1 e^{-t/\tau_1} + k_2 e^{-t/\tau_2}\right). \tag{4}$$

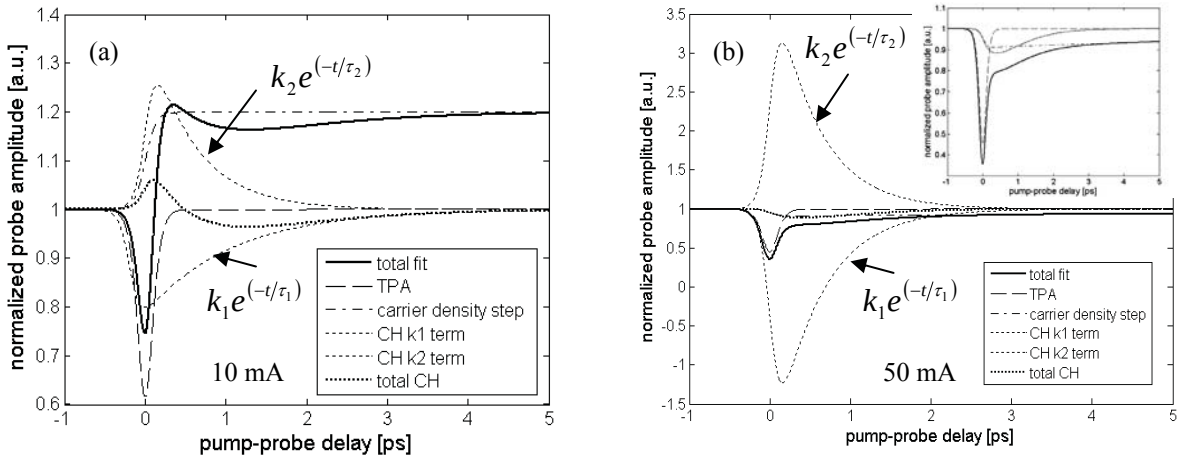

Figure 7 – Breakdown of fits at (a) 10 mA and (b) 50 mA showing the contribution of each ultrafast process from Equation (1). Inset of (b) shows a magnification of the 50 mA fit showing only the TPA, step, and total CH components.

The change in probe transmission measured in the experiments is then the impulse response *h(t)* convolved with the autocorrelation trace of the pump and probe pulses, *S(t)*:

$$\Delta T(\tau) = \int_{\infty}^{\infty} h(\tau - t) S(t) dt \,. \tag{5}$$

In Equations (1)-(4), the total impulse response *h(t)* is a sum of an instantaneous (delta-function) TPA response h_{TPA}, a step response due to the long-term carrier density change h_{cr}, and a bi-exponential carrier heating response h_{ch} which accounts for the carrier heating and consequent carrier cooling dynamic. Each component is multiplied by a unit step function at zero delay to make the system causal. In (4) k_1 and τ_1 account for the negative exponential decay (k_1 is always < 0), and k_2 and τ_2 the positive decay, which together give the carrier heating dynamic. In the fitting it was found that - $k_1 = k_2$ for all cases, such that (4) can be rewritten as:

$$h_{ch} = u(t) k_2 e^{-t/\tau_2} \left(1 - e^{-t/\tau_{eff}}\right), \tag{6}$$

where $1/\tau_{eff} = 1/\tau_1 - 1/\tau_2$. In this form the CH dynamic can now be identified as an initial fast carrier heating to the hot Fermi distribution with time constant τ_{eff} followed by a cooling back to the lattice temperature with time constant τ_2.

By varying the k_{TPA}, k_1, k_2, τ_1, *and* τ_2 values in the impulse response of Equation (1), and convolving it with a hyperbolic secant autocorrelation trace with FWHM = 0.230 ps for the 150 fs laser pulse, excellent fits were obtained for all of the short-term gain response curves, as seen in Figure 5 (b). Figure 7 shows a breakdown of the fitting for the 10mA and 50mA curves, illustrating the contributions of each of the ultrafast components in Equation (1). Values of τ_1 = 0.5 ps and τ_2 = 0.5-2.5 ps were found (see Figure 6 (b)), corresponding to $\tau_2 \approx 1.5$ ps and $\tau_{eff} \approx 0.75$ ps for the carrier heating and carrier cooling time constants, respectively. These lifetimes are again very similar to the carrier heating lifetimes observed in other semiconductor structures in the literature.

4. DISCUSSION

The results show some important characteristics of our 1.55 μm InAs/InGaAsP QD SOAs relevant for ultrafast signal processing. Firstly the fast 13.2 ps gain recovery observed corresponds theoretically to a 75 GHz switching rate limit, making the device promising as an ultrafast switching element. Secondly, a fast gain dynamic compared to the much slower (~ 500 ps) absorption dynamic matches observations made on an InAs/AlGaAs 1.3 μm QD SOA in [16], where similar heterodyne measurements revealed a 660 ps absorption recovery time and a 5.7 ps gain recovery time. Our 13.2 ps time constant here suggests the refilling of the dot ground states in the gain regime occurs via phonon-assisted relaxation, since this process is what is also attributed to the 5.7 ps value in [16]. Furthermore the similarity of our carrier recovery dynamics to this higher-confinement InAs/AlGaAs QD device reinforces that high quantum confinement has also been achieved in our 1.55 μm InAs/InGaAsP dots, as suggested in [19].

Our ultrafast dynamics consistent with carrier heating are similar to those measured for InGaAs/InGaAsP quantum well SOAs in [2]. The values of τ_2 = 0.5-2.5 ps and τ_1 = 0.5 ps are similar to, but slightly longer than the values of τ_2 = 0.6 ps and τ_1 = 0.2 ps reported in [2]. Comparing Figure 5 (b) and Figure 4, the strength of the carrier heating dynamics also appear similar. Strong carrier heating features however are in contrast to the results reported for the QD SOAs in [15], which showed carrier heating responses with similar lifetimes, but significantly reduced in magnitude. Here the reduction in carrier heating was attributed to a reduction in free carrier absorption (FCA) in QDs compared to quantum well or bulk structures. Ultrafast dynamics with reduced magnitudes are preferred for achieving cleaner ultrafast switching, thus further work could be done to reduce the strength of the carrier heating dynamics in these devices. Additional analysis of the carrier heating dynamics and discussion of the physical mechanisms behind the ultrafast carrier dynamics in these QD structures will be presented in a future report along with the measured phase dynamics.

5. CONCLUSIONS

We have characterized the ultrafast gain and carrier recovery dynamics of a novel 1.55 μm InAs/InGaAsP QD SOA using the heterodyne pump-probe experimental technique with a resolution of 150 fs. The heterodyne pump-probe experiments allow polarization and wavelength independent, cross-talk free measurement of both gain and refractive index temporal dynamics. The device showed a fast 13.2 ps gain recovery at 50 mA, making it promising for ultrafast switching at rates of >40 GHz. Strong carrier heating dynamics were also observed with time constants similar to those in previously reported devices. The measurements represent the first characterization of the temporal dynamics of a QD SOA operating in the 1.55 μm telecommunications wavelength range, and this device represents the only QD-based SOA reported to our knowledge capable of ≈100 GHz switching speeds which operates at these wavelengths.

6. REFERENCES

[1] C. N. Allen, P. J. Poole, P. Marshall, J. Fraser, S. Raymond, and S. Fafard, "InAs self-assembled quantum-dot lasers grown on (100) InP," Appl Phys Lett **80** (19), 3629-3631 (2002).

[2] K. L. Hall, G. Lenz, A. M. Darwish, and E. P. Ippen, "Subpicosecond Gain and Index Nonlinearities in InGaAsP Diode-Lasers," Opt Commun **111** (5-6), 589-612 (1994).

[3] M. Sugawara, H. Ebe, N. Hatori, M. Ishida, Y. Arakawa, T. Akiyama, K. Otsubo, and Y. Nakata, "Theory of optical signal amplification and processing by quantum-dot semiconductor optical amplifiers," Phys Rev B **69** (23), - (2004).

[4] M. Sugawara, T. Akiyama, N. Hatori, Y. Nakata, H. Ebe, and H. Ishikawa, "Quantum-dot semiconductor optical amplifiers for high-bit-rate signal processing up to 160 Gb/s and a new scheme of 3R regenerators," Meas Sci Technol **13** (11), 1683-1691 (2002).

[5] M. Sugawara, N. Hatori, T. Akiyama, Y. Nakata, and H. Ishikawa, "Quantum-dot semiconductor optical amplifiers for high bit-rate signal processing over 40 Gbit/s," Jpn J Appl Phys 2 **40** (5B), L488-L491 (2001).

[6] T. Akiyama, N. Hatori, Y. Nakata, H. Ebe, and M. Sugawara, "Pattern-effect-free amplification and cross-gain modulation achieved by using ultrafast gain nonlinearity in quantum-dot semiconductor optical amplifiers," Phys Status Solidi B **238** (2), 301-304 (2003).

[7] A. V. Uskov, J. Mork, B. Tromborg, T. W. Berg, I. Magnusdottir, and E. P. O'Reilly, "On high-speed cross-gain modulation without pattern effects in quantum dot semiconductor optical amplifiers," Opt Commun **227** (4-6), 363-369 (2003).
[8] A. V. Uskov, E. P. O'Reilly, R. J. Manning, R. P. Webb, D. Cotter, M. Laemmlin, N. N. Ledentsov, and D. Bimberg, "On ultrafast optical switching based on quantum-dot semiconductor optical amplifiers in nonlinear interferometers," IEEE Photonic Tech L **16** (5), 1265-1267 (2004).
[9] T. Akiyama, H. Kuwatsuka, N. Hatori, Y. Nakata, H. Ebe, and M. Sugawara, "Symmetric highly efficient (similar to 0 dB) wavelength conversion based on four-wave mixing in quantum dot optical amplifiers," IEEE Photonic Tech L **14** (8), 1139-1141 (2002).
[10] V. M. Ustinov, A. E. Zhukov, A. U. Egorov, and N. A. Maleev, *Quantum Dot Lasers*. (Oxford University Press, Oxford, 2003).
[11] K. I. Kang, I. Glesk, and P. R. Prucnal, *Ultrafast Optical Time Demultiplexers Using Semiconductor Optical Amplifiers*. (World Scientific: USA, 1996).
[12] N. S. Patel, K. L. Hall, and K. A. Rauschenbach, "Interferometric all-optical switches for ultrafast signal processing," Appl Optics **37** (14), 2831-2842 (1998).
[13] J. Leuthold, C. H. Joyner, B. Mikkelsen, G. Raybon, J. L. Pleumeekers, B. I. Miller, K. Dreyer, and C. A. Burrus, "100 Gbit/s all-optical wavelength conversion with integrated SOA delayed-interference configuration," Electron Lett **36** (13), 1129-1130 (2000).
[14] J. Leuthold, B. Mikkelsen, G. Raybon, C. H. Joyner, J. L. Pleumeekers, B. I. Miller, K. Dreyer, and R. Behringer, "All-optical wavelength conversion between 10 and 100 Gb/s with SOA delayed-interference configuration," Opt Quant Electron **33** (7-10), 939-952 (2001).
[15] P. Borri, W. Langbein, J. M. Hvam, F. Heinrichsdorff, M. H. Mao, and D. Bimberg, "Spectral hole-burning and carrier-heating dynamics in InGaAs quantum-dot amplifiers," IEEE J Sel Top Quant **6** (3), 544-551 (2000).
[16] P. Borri, S. Schneider, W. Langbein, U. Woggon, A. E. Zhukov, V. M. Ustinov, N. N. Ledentsov, Z. I. Alferov, D. Ouyang, and D. Bimberg, "Ultrafast carrier dynamics and dephasing in InAs quantum-dot amplifiers emitting near 1.3-um-wavelength at room temperature," Appl Phys Lett **79** (16), 2633-2635 (2001).
[17] K. L. Hall, Y. Lai, E. P. Ippen, G. Eisenstein, and U. Koren, "Femtosecond Gain Dynamics and Saturation Behavior in InGaAsP Multiple Quantum-Well Optical Amplifiers," Appl Phys Lett **57** (27), 2888-2890 (1990).
[18] S. Weiss, J. M. Wiesenfeld, D. S. Chemla, G. Raybon, G. Sucha, M. Wegener, G. Eisenstein, C. A. Burrus, A. G. Dentai, U. Koren, B. I. Miller, H. Temkin, R. A. Logan, and T. Tanbunek, "Carrier Capture Times in 1.5 um Multiple Quantum-Well Optical Amplifiers," Appl Phys Lett **60** (1), 9-11 (1992).
[19] C. N. Allen, P. J. Poole, P. Barrios, P. Marshall, G. Pakulski, S. Raymond, and S. Fafard, "External cavity quantum dot tunable laser through 1.55 mu m," Physica E **26** (1-4), 372-376 (2005).
[20] P. Borri, W. Langbein, J. M. Hvam, E. Heinrichsdorff, M. H. Mao, and D. Bimberg, "Ultrafast gain dynamics in InAs-InGaAs quantum-dot amplifiers," IEEE Photonic Tech L **12** (6), 594-596 (2000).
[21] K. L. Hall, G. Lenz, E. P. Ippen, and G. Raybon, "Heterodyne Pump Probe Technique for Time-Domain Studies of Optical Nonlinearities in Wave-Guides," Opt Lett **17** (12), 874-876 (1992).
[22] K. L. Hall, G. Lenz, E. P. Ippen, U. Koren, and G. Raybon, "Carrier Heating and Spectral Hole Burning in Strained-Layer Quantum-Well Laser-Amplifiers at 1.5-um," Appl Phys Lett **61** (21), 2512-2514 (1992).
[23] P. Borri, W. Langbein, J. Mork, and J. M. Hvam, "Heterodyne pump-probe and four-wave mixing in semiconductor optical amplifiers using balanced lock-in detection," Opt Commun **169** (1-6), 317-324 (1999).
[24] S.Schneider, U. Woggon, P. Borri, W. Langbein, D. Ouyang, R.L. Sellin, and D. Bimberg, presented at the CLEO 2005, Baltimore, MD, USA, 2005.
[25] P. Borri, W. Langbein, S. Schneider, U. Woggon, R. L. Sellin, D. Ouyang, and D. Bimberg, "Exciton relaxation and dephasing in quantum-dot amplifiers from room to cryogenic temperature," IEEE J Sel Top Quant **8** (5), 984-991 (2002).
[26] C. K. Sun, B. Golubovic, J. G. Fujimoto, H. K. Choi, and C. A. Wang, "Heterodyne Nondegenerate Pump-Probe Measurement Technique for Guided-Wave Devices," Opt Lett **20** (2), 210-212 (1995).
[27] M. Hofmann, S. D. Brorson, J. Mork, and A. Mecozzi, "Time resolved four-wave mixing technique to measure the ultrafast coherent dynamics in semiconductor optical amplifiers," Appl Phys Lett **68** (23), 3236-3238 (1996).
[28] A. Mecozzi and J. Mork, "Theory of heterodyne pump-probe experiments with femtosecond pulses," J Opt Soc Am B **13** (11), 2437-2452 (1996).
[29] K. L. Hall, E. T. Thoen, and E. P. Ippen, in *Semiconductors and Semimetals*, edited by E. Garmire and A. Kost (Academic Press, San Diego, 1999), Vol. 59: Nonlinear Optics in Semiconductors II.